Cavity-Enhanced Transport of Charge

David Hagenmüller,[1] Johannes Schachenmayer,[1] Stefan Schütz,[1] Claudiu Genes,[1,2] and Guido Pupillo[1]
[1]IPCMS (UMR 7504) and ISIS (UMR 7006), University of Strasbourg and CNRS, 67000 Strasbourg, France
[2]Max Planck Institute for the Science of Light, Staudtstraße 2, D-91058 Erlangen, Germany

(Received 2 March 2017; published 28 November 2017)

We theoretically investigate charge transport through electronic bands of a mesoscopic one-dimensional system, where interband transitions are coupled to a confined cavity mode, initially prepared close to its vacuum. This coupling leads to light-matter hybridization where the dressed fermionic bands interact via absorption and emission of dressed cavity photons. Using a self-consistent nonequilibrium Green's function method, we compute electronic transmissions and cavity photon spectra and demonstrate how light-matter coupling can lead to an enhancement of charge conductivity in the steady state. We find that depending on cavity loss rate, electronic bandwidth, and coupling strength, the dynamics involves either an individual or a collective response of Bloch states, and we explain how this affects the current enhancement. We show that the charge conductivity enhancement can reach orders of magnitudes under experimentally relevant conditions.

DOI: 10.1103/PhysRevLett.119.223601

The study of strong light-matter interactions [1–4] is playing an increasingly crucial role in understanding as well as engineering new states of matter with relevance to the fields of quantum optics [5–18], solid state physics [19–31], as well as quantum chemistry [32–36] and material science [37–53]. An emerging topic of interest is the modification of material properties using either external electromagnetic radiation [54–56] or spatially confined modes such as in cavity quantum electrodynamics [57–63]. Recent experiments with organic semiconductors have demonstrated a dramatic enhancement of charge conductivity when molecules interact strongly with a surface plasmon mode [64]. In principle, this can open up exciting new opportunities both for basic science and applications of organic electronics [65]. The microscopic mechanisms leading to charge conductivity enhancement, however, remain today largely unexplained. In this work, we propose a proof-of-principle model that sheds light on the physical mechanisms behind current enhancement due to the interaction with a confined bosonic mode. We show that our model can lead to a dramatic current enhancement by orders of magnitude for certain conditions that can be relevant to typical experiments across fields.

The setup we consider [see Fig. 1(a)] consists of a mesoscopic chain of N sites with two orbitals of energy ω_1 and ω_2 ($\hbar = 1$) in a 1D geometry, forming two bands in a tight-binding picture. The edges of the chain are connected to a source and a drain with a bias voltage across, respectively, inserting and removing (spinless) electrons in the two orbitals at rates Γ_1 and Γ_2. The on-site electronic transitions with energy $\omega_{21} = \omega_2 - \omega_1$ are resonantly coupled to a single cavity mode with coupling strength g and loss rate κ. Initially, we only allow electrons in the upper band to hop with a rate $t_2 \equiv t$, while no hopping is assumed in the lower band ($t_1 = 0$). Furthermore, we start with a situation of a large bias voltage, such that the Fermi level of the source (the drain) is higher (lower) than any other energy scale in the system, allowing for injection and extraction in both bands at a rate $\Gamma_1 = \Gamma_2 \equiv \Gamma$. Our single-mode model is justified as long as the coupling parameters g, κ and the electronic bandwidth $4t_2$ are small compared to the energy separation between the cavity modes, which in the resonant case is $\sim\omega_{21}$ [66].

In the case $g = 0$ [Fig. 1(b)] electronic transmission can only arise due to the bare upper-band Bloch states. We find that for $g \neq 0$ [Fig. 1(c)], the states of the two bands and the cavity mode hybridize to new states with enhanced transmission properties. Effectively, this results from a restoration

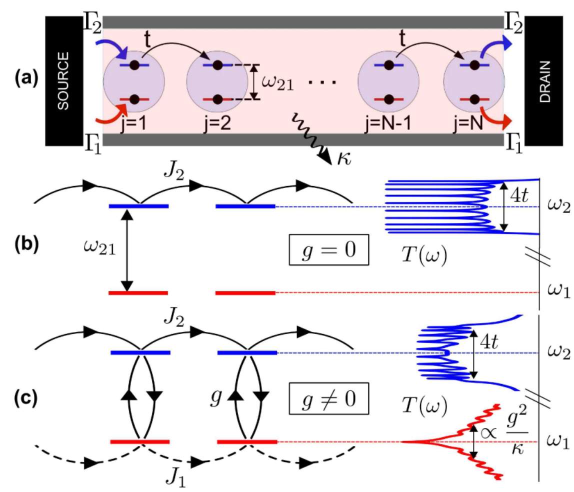

FIG. 1. (a) Model for 1D charge transport in the presence of a cavity. (b) In the absence of light-matter coupling, the hopping t allows for transmission in the upper band only. (c) In the presence of light-matter coupling (coupling strength g, photon loss rate κ), current can effectively flow through the two dressed bands (the currents J_1 and J_2 are defined in the text) providing a new contribution of width $\propto g^2/\kappa$ in the transmission spectrum $T(\omega)$.

of tunneling through the previously blocked lower band. More precisely, we show that the current enhancement is determined by the photon spectral weight present within the electronic bandwidth, which enables hybridization between the lower and the upper band Bloch states. In contrast to the usual Tavis-Cummings (TC) model for spins [68], where the system properties are determined by the ratio g/κ only, here, the nature of the light-matter coupling and that of the current enhancement also crucially depends on the ratios $\kappa/4t$ and $g/4t$ ($4t$ is the electronic bandwidth). We show that when $\kappa, g \ll 4t$, the hybridized states retain a well-defined quasi-momemtum, and the current enhancement can be interpreted as an effective hopping mechanism [sketched in Fig. 1(c)]. When the band dressing becomes collective (e.g. for $\kappa \gg 4t$, or $\kappa \ll 4t$ and $g \gg 4t$), damped oscillations of the charge density between the two bands associated with polariton states play an important role, a process that does not contribute to intersite charge transport. Finally, we show that the characteristics mentioned above can be identified in the cavity photon spectrum and could be directly accessed in absorption spectroscopy experiments.

The steady-state current J can be computed through the electronic transmission spectrum $T(\omega)$ as

$$J = \frac{e\Gamma}{2}\int \frac{d\omega}{2\pi} T(\omega), \qquad (1)$$

with ω the frequency and e the electron charge. The dressing of the electronic bands and the cavity mode requires a self-consistent solution of the problem, which we obtain using a nonequilibrium Green's function method [67,69–78]. For $g \neq 0$, we show that $T(\omega)$ acquires a new transmission channel [sketched in Fig. 1(c)], which is responsible for the current enhancement.

We consider the Hamiltonian $H_S = H_{\rm el} + H_{\rm int} + H_{\rm cav}$, where

$$H_{\rm el} = \sum_{j=1}^{N}\sum_{\alpha=1}^{2} \omega_\alpha c^\dagger_{\alpha,j} c_{\alpha,j} - t\sum_{j=1}^{N-1}(c^\dagger_{2,j+1}c_{2,j} + \text{H.c.}), \qquad (2)$$

$$H_{\rm int} = g\sum_{j=1}^{N}(c^\dagger_{2,j}c_{1,j}a + c^\dagger_{1,j}c_{2,j}a^\dagger), \qquad (3)$$

and $H_{\rm cav} = \omega_{21} a^\dagger a$. Here, a is the bosonic annihilation operator for the cavity mode, while the fermionic operator $c_{\alpha,j}$ annihilates an electron in the orbital $\alpha = 1, 2$ on site j. The term $H_{\rm el}$ (2) is diagonalized in k-space as $H_{\rm el} = \sum_{\alpha,k}\omega_{\alpha,k}\tilde{c}^\dagger_{\alpha,k}\tilde{c}_{\alpha,k}$, with $\omega_{2,k} = \omega_2 - 2t\cos[\pi k/(N+1)]$ and $\omega_{1,k} = \omega_1$. The Hamiltonian H_S can be thus partitioned into a diagonal part $H_0 = H_{\rm el} + H_{\rm cav}$ with known eigenstates, and the light-matter interaction (3) which is treated perturbatively. In the following, all energies are in units of ω_{21}, which is set to 1. In the high-bias regime, the transmission function entering Eq. (1) is derived as (see Supplemental Material [67])

$$T(\omega) = \mathbf{Tr}[\underline{\sigma}^1 \circ \underline{A}_\alpha(\omega) + (\underline{\sigma}^N - \underline{\sigma}^1)\circ \Im \underline{G}^<_\alpha(\omega)]. \qquad (4)$$

Here, $\mathbf{Tr} \equiv \sum_{\alpha,k,k'}$, underlined quantities denote $N\times N$ matrices, $\circ$ is the element-wise Hadamard product, $\Im$ stands for imaginary part, and $\underline{\sigma}^j$ is a matrix of Fourier coefficients [67]. Equations (1) and (4) correspond to a generalization of the Landauer formula [79] to nonequilibrium mesoscopic systems [75].

The first contribution of Eq. (4) involves the trace of the electron spectral function $\underline{A}_\alpha(\omega)$, proportional to the electron density of states (DOS) [67]. Similarly, a cavity photon DOS $A_c(\omega)$ can be introduced, which can be directly accessed experimentally by measuring the cavity absorption spectrum. As implied by the spectral function normalization $\int d\omega A_{\alpha,k,k'}(\omega) = 2\pi\delta_{k,k'}$, the effect of light-matter interactions on the steady-state current is entirely determined by the second term in Eq. (4), proportional to the trace of the "lesser" Green's function $\underline{G}^<_\alpha(\omega)$. The transmission spectrum and the expectation value of the electron populations $n_{\alpha,j} = \langle c^\dagger_{\alpha,j}c_{\alpha,j}\rangle$ can be computed in the framework of the self-consistent Born approximation [67,76].

In the absence of light-matter coupling ($g = 0$), the steady-state current flowing through the upper band is entirely driven by the ratio t/Γ [67,80]:

$$J = \frac{e\Gamma/2}{1 + (\Gamma/2t)^2}. \qquad (5)$$

When $t \ll \Gamma$, the current vanishes as $J \sim 2et^2/\Gamma$, while it reaches its maximum of $e\Gamma/2$ when $t \gg \Gamma$. In the latter regime, $T(\omega)$ consists of N well-resolved peaks of width $\propto \Gamma$ associated with the different Bloch states [69,70,73,77,81] [see Fig. 1(b)]. In the following, we focus on $t \gg \Gamma$ and $g \neq 0$.

In the presence of light-matter coupling, we find that the electron DOS is redistributed among the two bands, modifying the transmission spectrum. In particular, $T(\omega)$ acquires a peak of width $\propto g^2/\kappa$, centered around the bare lower band energy ω_1. As shown in [67], this scaling can be explained by an analytical calculation up to second order in the perturbation (3). Note that our method is exact in the perturbative regime $g^2/\kappa \ll \Gamma$, and $\kappa, g \ll \omega_{21}$. Nevertheless, we find qualitatively correct results even for $g^2/\kappa > \Gamma$ (as seen by comparisons with master equation simulations). Using our nonequilibrium Green's functions method, we now identify the microscopic mechanisms giving rise to the modified charge transmission properties in two distinct regimes.

We denote the case where $\kappa, g \ll 4t$ as "individual dressing regime." This situation is depicted in Fig. 2 for an example with $N = 30$, $\Gamma = 2.5\times10^{-4}$, $t = 0.07$, and $\kappa = 5\times10^{-3}$. Figure 2(a) displays the steady-state cavity photon DOS (for $g = 0.03$), which we find to be a key quantity to explore the interplay between charge transport and strong coupling physics. In this regime, the narrow bare

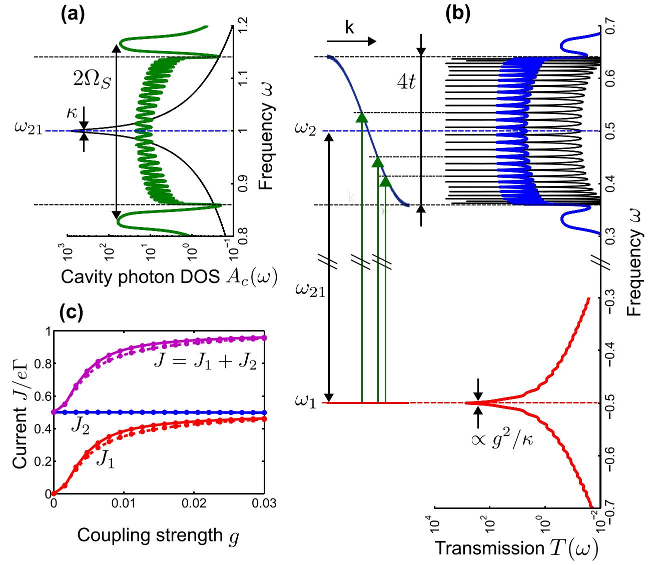

FIG. 2. "Individual dressing regime," with $\Gamma = 2.5 \times 10^{-4}$, $t = 0.07$, and $\kappa = 5 \times 10^{-3}$. (a) (Log-scale) cavity photon density of state $A_c(\omega)$ for $N = 30$. The thin black line corresponds to the bare cavity mode ($g = 0$), and the green line to the dressed one ($g = 0.03$). (b) (Log-scale) transmission function $T(\omega)$ for $N = 30$. The thin black line corresponds to $g = 0$, while the red and blue lines correspond, respectively, to the vicinity of the lower ($\sim\omega_1 = -0.5$) and the upper band ($\sim\omega_2 = 0.5$) for $g = 0.03$. The Bloch states dispersion is plotted on the left side of (b), and a few interband transitions are depicted as vertical green arrows. (c) Currents versus coupling strength g for $N = 10$ (solid) and $N = 30$ (dashed). Red, blue, and magenta lines represent the partial currents J_1, J_2, and the total current J (see text).

cavity mode (thin black line) is resonant with only a few interband transitions (with frequencies $\omega_{2,k} - \omega_1$) between the lower and the upper band Bloch states. We find that when g is larger than the separation between adjacent Bloch states, two polariton peaks separated by a splitting $2\Omega_S$ appear outside the electronic bandwidth, while inside the bandwidth, we clearly resolve $N - 1$ peaks associated with interband transitions [82].

The transmission spectrum $T(\omega)$ is shown in Fig. 2(b) for $g = 0$ (black line) and $g = 0.03$ (blue and red lines). The key feature is the appearance of the large peak of width $\propto g^2/\kappa$ centered at the bare flat band energy ω_1 for $g \neq 0$. This peak originates from interband electronic transitions concurrently with the absorption and emission of cavity photons with energy $\omega \approx \omega_{21}$. This new transmission corresponds to the opening of a transport channel with effective hopping rate $\propto g^2/\kappa$, responsible for the observed current enhancement. Note that the peaked structure of the upper-band Bloch states still remains visible in $T(\omega)$ for $g \neq 0$. This indicates that a well-defined quasimomentum can still be associated with the dressed Bloch states, which supports the coherent effective hopping picture. The two polariton peaks from the cavity photon DOS give rise to only marginal contributions outside the bandwidth $4t$ (note the logscale).

Figure 2(c) shows the effective currents J_1 and J_2 as a function of g, which are obtained by integrating $T(\omega)$ in the vicinity of ω_1 and ω_2, respectively. The effective lower band current J_1 results from the new channel appearing around ω_1 and strongly increases in the considered range of g. Crucially, in this individual dressing regime, the current J_2 is barely affected by the coupling, and we find that the currents are nearly independent of the chain length N. The overall current $J = J_1 + J_2$ [83] reaches its maximum $e\Gamma$ asymptotically for large g.

The "collective dressing regime" is typically achieved when $\kappa \gg 4t$. This is depicted in Fig. 3 for an example with $N = 30$, $\Gamma = 2.5 \times 10^{-4}$, $t = 2.5 \times 10^{-3}$, and $\kappa = 0.05$. Figure 3(a) displays the cavity DOS. Here, for $g = 0$, the broad bare cavity mode of width κ (thin black line) is resonant to all interband transitions. The photon DOS in the coupled case with $g = 0.03$ is shown as a thick green line. The small peak centered at ω_{21} now consists of $N - 1$ overlapping peaks (not resolved) with small photon weight. In this situation, we again observe two polariton peaks outside the electronic bandwidth, but in contrast to Fig. 2(a), they concentrate most of the photon spectral weight, which reduces the individual band dressing. Here, the dynamics is dominated by collective oscillations of the charge density at a frequency Ω_S, as discussed below.

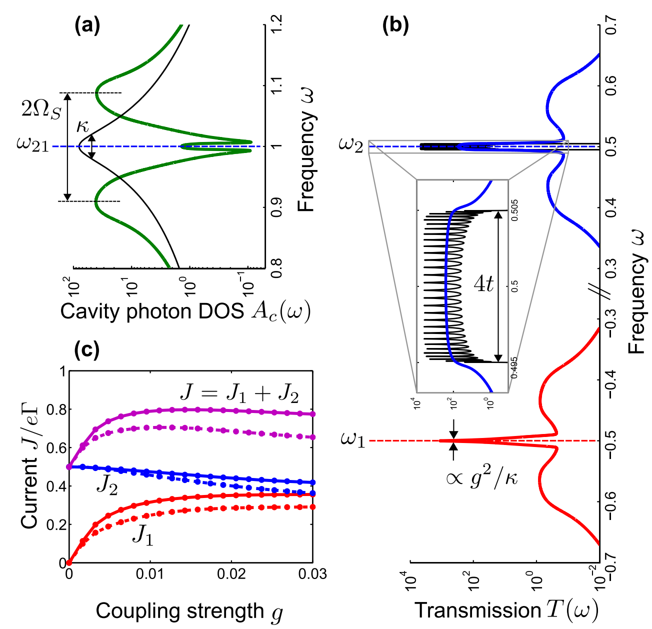

FIG. 3. "Collective dressing regime." Same quantities as in Fig. 2 for $\Gamma = 2.5 \times 10^{-4}$, $t = 2.5 \times 10^{-3}$, and $\kappa = 0.05$. N and g are identical to Fig. 2. (a) (Log-scale) cavity photon density of state $A_c(\omega)$. (b) (Log-scale) transmission function $T(\omega)$. The central region is shown in the inset. (c) Partial and total currents versus coupling strength g.

The transmission spectrum $T(\omega)$ in the steady-state is shown in Fig. 3(b) for $g = 0$ (thin black line, inset) and $g = 0.03$ (blue and red lines). Again, we observe large peaks around ω_1 (red) and ω_2 (blue). In contrast to Fig. 2, the peaked structure associated with the individual band dressing disappears, indicating a collective response of the Bloch states that cannot be associated with a well-defined quasimomentum (see inset).

In Fig. 3(c), we observe that this collective behavior leads to an upper band current J_2 decreasing with g, and resulting in a maximum in the overall current. This feature can be intuitively understood, as damped collective oscillations remove populations from the upper band. Furthermore, we find that J decreases significantly when increasing the chain length N, which is another indication of the presence of collective effects (i.e. the relevant coupling parameter is Ω_S and not g [67]). These features will be further addressed in [84].

Our open system exhibits a larger Hilbert space (4^N) compared to the usual TC model for spins (2^N). The latter can be recovered only by constraining the electron number to one for each two-level system, providing a splitting $2g\sqrt{N}$ between the two polaritons [68]. In our two-band model, a collective vacuum Rabi splitting can be defined as $\Omega_n = g\sqrt{N_1 - N_2}$ ($N_\alpha = \sum_j n_{\alpha,j}$) [85], which is obtained from the steady-state population imbalance between the two bands. Importantly, since sites with both orbitals occupied (or empty) are not effectively coupled to light, we always find $\Omega_n < g\sqrt{N}$, which implies that the TC model cannot be used to determine, e.g., the number of molecules based on measured Ω_S in experiments. In general, $\Omega_n \approx \Omega_S$ is an indication of the presence of collective effects associated with joint charge oscillations between the two bands. This is the case in Fig. 3; however, we expect that this dynamics can also be recovered in the regime where $\kappa \ll 4t$ and $g \gg 4t$, i.e. when g is large enough to couple all the Bloch states together (see [67]).

Having identified the current enhancement mechanisms, we now consider a scenario more reminiscent of typical experiments. Different overlaps between the electronic states of the leads and the systems' orbitals generally lead to a situation where $\Gamma_1 \neq \Gamma_2$. Now, we further assume a small finite hopping between the lower orbitals leading to an additional Hamiltonian term $-t_1 \sum_{j=1}^{N-1} (c^\dagger_{1,j+1} c_{1,j} + \text{H.c.})$, with $t_1 \ll \Gamma_1$. We choose $t_2 \gg t_1$ as spatially extended upper orbitals generally exhibit larger overlaps than valence orbitals. In an asymmetric situation, where one has a poor injection and extraction rate in the upper band with large hopping, and vice versa for the lower band, photon dressing of the two bands then allows for dramatic current enhancement. Now, the total current has two contributions even for $g = 0$, and still considering $t_2 \gg \Gamma_2$, Eq. (5) is extended to $J = (e\Gamma_1/2)[(2t_1/\Gamma_1)^2 + \Gamma_2/\Gamma_1]$. While previously the second term was $\Gamma_2/\Gamma_1 = 1$, now $\Gamma_2/\Gamma_1 \ll 1$, and for $g \neq 0$, the current restored in the lower band becomes the dominant contribution. Ultimately, when $t_1 \ll \Gamma_1$, the relative current enhancement is only limited by the ratio Γ_1/Γ_2 [67]. We note that the limit $\Gamma_2 \to 0$ is equivalent to the low-bias regime (when the Fermi level at zero-voltage lies in the lower band), where electrons can only be injected and extracted in the lower band.

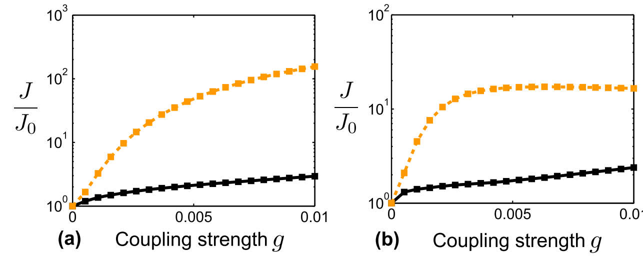

FIG. 4. Current enhancement J/J_0 (J_0 is the current for $g = 0$) versus g. (a) Individual dressing regime with $t = 0.07$, $\Gamma_1 = 0.01$, and $\kappa = 5 \times 10^{-3}$. (b) Collective dressing regime with $t = 2.5 \times 10^{-3}$, $\Gamma_1 = 10^{-3}$, and $\kappa = 0.05$. The full black and dotted orange lines correspond to $N_{\text{ph}} = 0$, 0.5, respectively. Other parameters are $N = 30$, $\Gamma_2 = 10^{-5}$, and $t_1 = 5 \times 10^{-5}$.

In a plausible scenario, electrons will also be injected into defect states which in turn can spontaneously decay and provide residual population in the photon bath. This residual population has a considerable effect, as e.g. for $\Gamma_2 \to 0$, it is needed to initiate the effective hopping process through the dressed bands. In Fig. 4, we show the current enhancement for mean photon population in the bath $N_{\text{ph}} = 0$, 0.5 and $\Gamma_2 \ll \Gamma_1$. Panels (a) and (b) display the individual and collective dressing regimes, respectively. Both panels demonstrate order-of-magnitude enhancements even for $N_{\text{ph}} \leq 1$, i.e. a cavity mode close to the vacuum. In both cases, increasing the photon population boosts the current significantly further. In [67], we show that the latter originates from a bosonic enhancement scaling as $g\sqrt{N_{\text{ph}}}$.

In this work, we introduced a proof-of-principle mechanism to enhance charge conductivity in a mesoscopic chain by coupling it to the vacuum field of a cavity. Our model might find applications in several fields, such as organic semiconductors [64], nanowires [86], carbon nanotubes [87], or quantum dot arrays [88,89]. In particular, pairs of quantum dots have recently been coupled to microwave cavities [29–31]. Possible extensions of our model include coupling to multiple transmission channels in different geometries, as well as the competition between light-matter coupling and Anderson localization in random lattices. Note that we expect our findings to qualitatively hold in the case of a direct generalization of our model to higher dimensions. The method used in this article provides new perspectives for the investigation of many-body systems strongly coupled to cavity resonances or other bosonic degrees of freedom.

We are grateful to Thibault Chervy, Roberta Citro, Thomas Ebbesen, Cyriaque Genet, Emanuele Orgiu, and

Paolo Samorì for inspiring discussions. Work in Strasbourg was supported by the ERC St-Grant ColDSIM (No. 307688), with additional funding from Rysq and ANR-FWF grant BLUESHIELD. C. G. acknowledges support from the Max Planck Society and from the COST action NQO 1403 (Nano-scale Quantum Optics). This work is supported by IdEx Unistra with funding managed by the French National Research Agency as part of the "Investments for the future" program.

[1] C. Weisbuch, M. Nishioka, A. Ishikawa, and Y. Arakawa, Phys. Rev. Lett. **69**, 3314 (1992).
[2] D. G. Lidzey, D. D. C. Bradley, M. S. Skolnick, T. Virgili, S. Walker, and D. M. Whittaker, Nature (London) **395**, 53 (1998).
[3] J. M. Raimond, M. Brune, and S. Haroche, Rev. Mod. Phys. **73**, 565 (2001).
[4] J. P. Reithmaier, G. Sek, A. Loffler, C. Hofmann, S. Kuhn, S. Reitzenstein, L. V. Keldysh, V. D. Kulakovskii, T. L. Reinecke, and A. Forchel, Nature (London) **432**, 197 (2004).
[5] T. Yoshie, A. Scherer, J. Hendrickson, G. Khitrova, H. M. Gibbs, G. Rupper, C. Ell, O. B. Shchekin, and D. G. Deppe, Nature (London) **432**, 200 (2004).
[6] S. Savasta, O. Di Stefano, V. Savona, and W. Langbein, Phys. Rev. Lett. **94**, 246401 (2005).
[7] I. Fushman, D. Englund, A. Faraon, N. Stoltz, P. Petroff, and J. Vučković, Science **320**, 769 (2008).
[8] S. I. Tsintzos, N. T. Pelekanos, G. Konstantinidis, Z. Hatzopoulos, and P. G. Savvidis, Nature (London) **453**, 372 (2008).
[9] K. G. Lagoudakis, M. Wouters, M. Richard, A. Baas, I. Carusotto, R. Andre, L. S. Dang, and B. Deveaud-Pledran, Nat. Phys. **4**, 706 (2008).
[10] J. Claudon, J. Bleuse, N. S. Malik, M. Bazin, P. Jaffrennou, N. Gregersen, C. Sauvan, P. Lalanne, and J.-M. Gerard, Nat. Photonics **4**, 174 (2010).
[11] S. Kena-Cohen and S. R. Forrest, Nat. Photonics **4**, 371 (2010).
[12] P. Cristofolini, G. Christmann, S. I. Tsintzos, G. Deligeorgis, G. Konstantinidis, Z. Hatzopoulos, P. G. Savvidis, and J. J. Baumberg, Science **336**, 704 (2012).
[13] F. Albert, K. Sivalertporn, J. Kasprzak, M. Strauß, C. Schneider, S. Höfling, M. Kamp, A. Forchel, S. Reitzenstein, E. A. Muljarov, and W. Langbein, Nat. Commun. **4**, 1747 (2013).
[14] C. Schneider, A. Rahimi-Iman, N. Y. Kim, J. Fischer, I. G. Savenko, M. Amthor, M. Lermer, A. Wolf, L. Worschech, V. D. Kulakovskii, I. A. Shelykh, M. Kamp, S. Reitzenstein, A. Forchel, Y. Yamamoto, and S. Hofling, Nature (London) **497**, 348 (2013).
[15] R. Yalla, M. Sadgrove, K. P. Nayak, and K. Hakuta, Phys. Rev. Lett. **113**, 143601 (2014).
[16] A. Goban, C.-L. Hung, J. D. Hood, S.-P. Yu, J. A. Muniz, O. Painter, and H. J. Kimble, Phys. Rev. Lett. **115**, 063601 (2015).
[17] A. Javadi, I. Söllner, M. Arcari, S. L. Hansen, L. Midolo, S. Mahmoodian, G. Kiršanské, T. Pregnolato, E. H. Lee, J. D. Song, S. Stobbe, and P. Lodahl, Nat. Commun. **6**, 8655 (2015).
[18] A. Sipahigil, R. E. Evans, D. D. Sukachev, M. J. Burek, J. Borregaard, M. K. Bhaskar, C. T. Nguyen, J. L. Pacheco, H. A. Atikian, C. Meuwly, R. M. Camacho, F. Jelezko, E. Bielejec, H. Park, M. Lončar, and M. D. Lukin, Science **354**, 847 (2016).
[19] A. Tredicucci, Y. Chen, V. Pellegrini, M. Börger, L. Sorba, F. Beltram, and F. Bassani, Phys. Rev. Lett. **75**, 3906 (1995).
[20] J. Kasprzak, M. Richard, S. Kundermann, A. Baas, P. Jeambrun, J. M. J. Keeling, F. M. Marchetti, M. H. Szymanska, R. Andre, J. L. Staehli, V. Savona, P. B. Littlewood, B. Deveaud, and L. S. Dang, Nature (London) **443**, 409 (2006).
[21] K. Hennessy, A. Badolato, M. Winger, D. Gerace, M. Atature, S. Gulde, S. Falt, E. L. Hu, and A. Imamoğlu, Nature (London) **445**, 896 (2007).
[22] A. Amo, D. Sanvitto, F. P. Laussy, D. Ballarini, E. d. Valle, M. D. Martin, A. Lemaitre, J. Bloch, D. N. Krizhanovskii, M. S. Skolnick, C. Tejedor, and L. Vina, Nature (London) **457**, 291 (2009).
[23] H. Deng, H. Haug, and Y. Yamamoto, Rev. Mod. Phys. **82**, 1489 (2010).
[24] I. Carusotto and C. Ciuti, Rev. Mod. Phys. **85**, 299 (2013).
[25] J. M. Ménard, C. Poellmann, M. Porer, U. Leierseder, E. Galopin, A. Lemaître, A. Amo, J. Bloch, and R. Huber, Nat. Commun. **5**, 4648 (2014).
[26] S. Smolka, W. Wuester, F. Haupt, S. Faelt, W. Wegscheider, and A. Imamoglu, Science **346**, 332 (2014).
[27] O. Cotleţ, S. Zeytinoğlu, M. Sigrist, E. Demler, and A. Imamoğlu, Phys. Rev. B **93**, 054510 (2016).
[28] S. Zeytinoğlu, A. Imamoğlu, and S. Huber, Phys. Rev. X **7**, 021041 (2017).
[29] Y.-Y. Liu, J. Stehlik, C. Eichler, M. J. Gullans, J. M. Taylor, and J. R. Petta, Science **347**, 285 (2015).
[30] T. Frey, P. J. Leek, M. Beck, A. Blais, T. Ihn, K. Ensslin, and A. Wallraff, Phys. Rev. Lett. **108**, 046807 (2012).
[31] J. J. Viennot, M. R. Delbecq, M. C. Dartiailh, A. Cottet, and T. Kontos, Phys. Rev. B **89**, 165404 (2014).
[32] A. Shalabney, J. George, J. A. Hutchison, G. Pupillo, C. Genet, and T. W. Ebbesen, Nat. Commun. **6**, 5981 (2015).
[33] J. George, A. Shalabney, J. A. Hutchison, C. Genet, and T. W. Ebbesen, J. Phys. Chem. Lett. **6**, 1027 (2015).
[34] F. Herrera and F. C. Spano, Phys. Rev. Lett. **116**, 238301 (2016).
[35] R. Chikkaraddy, B. de Nijs, F. Benz, S. J. Barrow, O. A. Scherman, E. Rosta, A. Demetriadou, P. Fox, O. Hess, and J. J. Baumberg, Nature (London) **535**, 127 (2016).
[36] J. Galego, F. J. Garcia-Vidal, and J. Feist, Nat. Commun. **7**, 13841 (2016).
[37] A. Badolato, K. Hennessy, M. Atatüre, J. Dreiser, E. Hu, P. M. Petroff, and A. Imamoğlu, Science **308**, 1158 (2005).
[38] J. R. Tischler, M. S. Bradley, V. Bulović, J. H. Song, and A. Nurmikko, Phys. Rev. Lett. **95**, 036401 (2005).
[39] A. V. Akimov, A. Mukherjee, C. L. Yu, D. E. Chang, A. S. Zibrov, P. R. Hemmer, H. Park, and M. D. Lukin, Nature (London) **450**, 402 (2007).
[40] L. Sapienza, A. Vasanelli, R. Colombelli, C. Ciuti, Y. Chassagneux, C. Manquest, U. Gennser, and C. Sirtori, Phys. Rev. Lett. **100**, 136806 (2008).
[41] S. Aberra Guebrou, C. Symonds, E. Homeyer, J. C. Plenet, Y. N. Gartstein, V. M. Agranovich, and J. Bellessa, Phys. Rev. Lett. **108**, 066401 (2012).

[42] P. Vasa, W. Wang, R. Pomraenke, M. Lammers, M. Maiuri, C. Manzoni, G. Cerullo, and C. Lienau, Nat. Photonics **7**, 128 (2013).
[43] A. González-Tudela, P. A. Huidobro, L. Martín-Moreno, C. Tejedor, and F. J. García-Vidal, Phys. Rev. Lett. **110**, 126801 (2013).
[44] D. Tanese, H. Flayac, D. Solnyshkov, A. Amo, A. Lemaître, E. Galopin, R. Braive, P. Senellart, I. Sagnes, G. Malpuech, and J. Bloch, Nat. Commun. **4**, 1749 (2013).
[45] D. Ballarini, M. De Giorgi, E. Cancellieri, R. Houdré, E. Giacobino, R. Cingolani, A. Bramati, G. Gigli, and D. Sanvitto, Nat. Commun. **4**, 1778 (2013).
[46] P. Bhattacharya, B. Xiao, A. Das, S. Bhowmick, and J. Heo, Phys. Rev. Lett. **110**, 206403 (2013).
[47] J. D. Plumhof, T. Stöferle, L. Mai, U. Scherf, and R. F. Mahrt, Nat. Mater. **13**, 247 (2014).
[48] L. Shi, T. K. Hakala, H. T. Rekola, J.-P. Martikainen, R. J. Moerland, and P. Törmä, Phys. Rev. Lett. **112**, 153002 (2014).
[49] X. Liu, T. Galfsky, Z. Sun, F. Xia, E.-c. Lin, Y.-H. Lee, S. Kéna-Cohen, and V. M. Menon, Nat. Photonics **9**, 30 (2015).
[50] T. U. Tumkur, G. Zhu, and M. A. Noginov, Opt. Express **24**, 3921 (2016).
[51] J. A. Ćwik, P. Kirton, S. De Liberato, and J. Keeling, Phys. Rev. A **93**, 033840 (2016).
[52] M. D. LaCount and M. T. Lusk, Phys. Rev. A **93**, 063811 (2016).
[53] R. T. Grant, P. Michetti, A. J. Musser, P. Gregoire, T. Virgili, E. Vella, M. Cavazzini, K. Georgiou, F. Galeotti, C. Clark, J. Clark, C. Silva, and D. G. Lidzey, Adv. Opt. Mater. **4**, 1615 (2016).
[54] M. Mitrano, A. Cantaluppi, D. Nicoletti, S. Kaiser, A. Perucchi, S. Lupi, P. Di Pietro, D. Pontiroli, M. Riccó, S. R. Clark, D. Jaksch, and A. Cavalleri, Nature (London) **530**, 461 (2016).
[55] S. Masayuki, R. Kato, and H. M. Yamamoto, Science **347**, 743 (2015).
[56] G. Mazza and A. Georges, Phys. Rev. B **96**, 064515 (2017).
[57] S. De Liberato and C. Ciuti, Phys. Rev. B **79**, 075317 (2009).
[58] F. P. Laussy, A. V. Kavokin, and I. A. Shelykh, Phys. Rev. Lett. **104**, 106402 (2010).
[59] S. Morina, O. V. Kibis, A. A. Pervishko, and I. A. Shelykh, Phys. Rev. B **91**, 155312 (2015).
[60] J. Feist and F. J. Garcia-Vidal, Phys. Rev. Lett. **114**, 196402 (2015).
[61] J. Schachenmayer, C. Genes, E. Tignone, and G. Pupillo, Phys. Rev. Lett. **114**, 196403 (2015).
[62] A. Kavokin and P. Lagoudakis, Nat. Mater. **15**, 599 (2016).
[63] V. Gudmundsson, N. R. Abdullah, A. Sitek, H.-S. Goan, C.-S. Tang, and A. Manolescu, Phys. Rev. B **95**, 195307 (2017).
[64] E. Orgiu, J. George, J. Hutchison, E. Devaux, J. F. Dayen, B. Doudin, F. F. Stellacci, C. Genet, J. Schachenmayer, C. Genes, G. Pupillo, P. Samori, and T. W. Ebbesen, Nat. Mater. **14**, 1123 (2015).
[65] A. Salleo, Nat. Mater. **14**, 1077 (2015).
[66] In [67], as an example, we show this explicitly for a waveguide design, where the electromagnetic field is confined in the two directions perpendicular to the chain axis, Phys. Rev. A 50, 1830 (1994).
[67] See Supplemental Material at http://link.aps.org/supplemental/10.1103/PhysRevLett.119.223601 for detailed calculations using nonequilibrium Green's function and quantum master equation methods.
[68] M. Tavis and F. W. Cummings, Phys. Rev. **170**, 379 (1968).
[69] C. Caroli, R. Combescot, P. Nozieres, and D. Saint-James, J. Phys. C **4**, 916 (1971).
[70] C. Caroli, R. Combescot, P. Nozieres, and D. Saint-James, J. Phys. C **5**, 21 (1972).
[71] J. L. D'Amato and H. M. Pastawski, Phys. Rev. B **41**, 7411 (1990).
[72] S. Datta, *Electronic Transport in Mesoscopic Systems:* (Cambridge University Press, Cambridge, MA, 1995).
[73] T.-S. Kim and S. Hershfield, Phys. Rev. B **65**, 214526 (2002).
[74] D. Roy and A. Dhar, Phys. Rev. B **75**, 195110 (2007).
[75] H. Haug and A.-P. Jauho, *Quantum Kinetics in Transport and Optics of Semiconductors* (Springer-Verlag, Berlin, Heidelberg, 2008).
[76] M. Pourfath, *The Non-Equilibrium Green's Function Method for Nanoscale Device Simulation* (Springer-Verlag, Wien, 2014).
[77] R. J. Doornenbal, G. Skantzaris, and H. T. C. Stoof, Phys. Rev. B **91**, 045419 (2015).
[78] D. Gruss, K. A. Velizhanin, and M. Zwolak, Sci. Rep. **6**, 24514 (2016).
[79] R. Landauer, Z. Phys. B **68**, 217 (1987).
[80] M. V. Medvedyeva and S. Kehrein, arXiv:1310.4997.
[81] A. Dhar, K. Saito, and P. Hänggi, Phys. Rev. E **85**, 011126 (2012).
[82] Some of the qualitative features of the cavity photon DOS follow from a simple generalization of the TC Hamiltonian [68]: $H_{\mathrm{TC}} = \omega_0 a^\dagger a + \sum_{k=1}^{N} (\omega_{2,k} - \omega_1)\sigma_k^z/2 + g\sum_k (\sigma_k^+ a + \sigma_k^- a^\dagger)$, where $\sigma_k^z, \sigma_k^\pm$ are the Pauli operators associated with the N interband transitions.
[83] Note that the overall current can be also obtained using a master equation approach as we detail in [67]. We find that the results are consistent with the nonequilibrium Green's functions method.
[84] D. Hagenmüller, S. Schütz, J. Schachenmayer, C. Genes, and G. Pupillo (to be published).
[85] Y. Todorov, A. M. Andrews, R. Colombelli, S. De Liberato, C. Ciuti, P. Klang, G. Strasser, and C. Sirtori, Phys. Rev. Lett. **105**, 196402 (2010).
[86] R. Rurali, Rev. Mod. Phys. **82**, 427 (2010).
[87] E. A. Laird, F. Kuemmeth, G. A. Steele, K. Grove-Rasmussen, J. Nygård, K. Flensberg, and L. P. Kouwenhoven, Rev. Mod. Phys. **87**, 703 (2015).
[88] Z. M. Wang, K. Holmes, Y. I. Mazur, and G. J. Salamo, Appl. Phys. Lett. **84**, 1931 (2004).
[89] C. R. Kagan and C. B. Murray, Nat. Nanotechnol. **10**, 1013 (2015).